Article

Reinforcement of Flexural Members with Basalt Fiber Mortar

Dmitry Kurlapov [1], Sergey Klyuev [2], Yury Biryukov [1], Nikolai Vatin [3], Dmitry Biryukov [1], Roman Fediuk [4,*] and Yuriy Vasilev [5]

1   Military Institute (Engineering) of the Military Academy of Logistics, 191123 St. Petersburg, Russia; Kurlapovdv@mail.ru (D.K.); uabiryukov@mail.ru (Y.B.); b_d_v0402@mail.ru (D.B.)
2   Belgorod State Technological University Named after V.G. Shukhov, 308012 Belgorod, Russia; Klyuyev@yandex.ru
3   Peter the Great St. Petersburg Polytechnic University, 195251 St. Petersburg, Russia; vatin@mail.ru
4   Polytechnic Institute, Far Eastern Federal University, 690922 Vladivostok, Russia
5   Department of Road-Building Materials, Moscow Automobile and Road Construction University, 125319 Moscow, Russia; yu.vasilev@madi.ru
*   Correspondence: roman44@yandex.ru

Abstract: Reconstruction of buildings and structures is becoming one of the main directions in the field of construction, and the design and production of works during reconstruction are significantly different from the ones of new buildings and structures. After carrying out a number of studies on the inspection of the technical condition of buildings in order to determine the effect of defects on the bearing capacity, the criteria for assessing the state of floor slab structures were identified. Conclusions on the state and further work of elements of reinforced concrete structures are considered. The authors achieve the aim of reinforcing flexural elements of reinforced concrete structures with fiber-reinforced mortar, which is especially important for floor elements with increased operational requirements. A technique for constructing a reinforcement layer using fiber-reinforced mortar from coarse basalt fiber has been developed. The parameters of basalt fiber in the reinforcement layer are substantiated. A method for solving problems of the operation of multilayer coatings under the influence of operational loads is used, in which the model prerequisites for describing the operation of layers are simplified, where the bearing layers are represented by classical Kirchhoff-Love plates. When solving problems, the maximum possible number of design features of flexural members is taken into account, in combination with appropriate experimental studies, the method allows us to consider all the variety of structures for reinforcing coatings and meet the needs of their practical application.

Keywords: mortar; fiber; structure; reinforcement; flexural members

1. Introduction

The design and production of work during the reconstruction differ significantly from the design and construction of new buildings and structures [1,2]. Before planning for the reconstruction of buildings and structures, it is necessary to carry out a competent examination of the technical condition [3]. According to regulatory documents, examination of the technical condition of buildings and structures is carried out at least once every 10 years and at least once every five years for buildings and structures or their individual elements operating in adverse conditions [4–10]. Based on the results of the survey, the actual bearing capacity and serviceability of building structures should be established in order to use these data in the development of a reinforcement project for reconstruction [11,12]. Also, a search should be carried out for the optimal variant of the structural and planning solution, a method for the possible strengthening of supporting structures, taking into account its manufacturability [2,13].

When reinforcing bending elements by increasing the section in the compressed zone of concrete, an important issue is to ensure the compatibility of the work of the old

concrete and new mortar [14,15]. When constructing transverse grooves and cutting the surface of old concrete, the laboriousness of this reinforcement method increases with large volumes of work (reinforcement of floor slabs. In the scientific literature there are a number of recommendations for the calculation of flexural reinforced concrete elements with dispersed reinforcement mortar [16,17]. In particular, Aghdasi and Ostertag [18] studied in detail the characteristics of tensile fracture of green ultra-high performance fiber-reinforced concrete. Taheri et al. [19] used an integrated approach to predicting crack width and distance between flexural elements made of FRC with hybrid reinforcement. Iranian scientists [20] conducted a comprehensive experimental study of bending and shear strengthening of reinforced concrete beams using self-reinforced concrete jackets reinforced with fiber. However to determine the magnitude of the compatibility of the work of old concrete and new mortar, additional experimental studies are required [21,22].

An effective and fairly simple way to strengthen the flexural members of industrial buildings is to install additional rigid supports in the form of struts or vertical elements. However, these solutions are limited by the conditions of the technological process, which does not allow constraining the dimensions of production facilities [23,24]. To reduce the bending moments in the elements of a multi-span multi-tiered frame, cross-prestressed ties of flexible metal strands can be used [25]. Other low-invasive and fast techniques for this purpose also find application in construction practice, for example, externally bonded, surface-mounted fiberglass composites. A less time-consuming method is reinforcement with vertical overhead clamps [26].

The main method of strengthening flexural reinforced concrete elements by increasing the bearing capacity of elements without changing the design scheme is the method of increasing the sections of elements [27]. Reinforced concrete flexural members (beams, girders, crane beams, slabs, floors and coverings) are reinforced by building up in height or width (from below, from the sides and from above of the reinforced element) [28]. A feature of this method is the perception of shear stresses acting in the plane of contact of old concrete with new mortar, special additional reinforcement welded to the reinforcement of the reinforced structure [29]. At present, to strengthen building members, in particular, flexural reinforced concrete elements, it is promising to use high-performance structural materials, for example, steel-fiber reinforced concrete, which surpasses fine-grained concrete in strength and deformation characteristics [30]. Two types of fiber used to strengthen reinforced concrete structures, polypropylene and steel, have been sufficiently investigated [31]. Polypropylene fiber improves the performance of concrete during its initial curing period [32]. Steel fiber improves the performance of concrete after the one has hardened. On the other hand, basalt fiber (BF) has the potential to improve the performance of concrete, both initially and thereafter [33,34]. The advantage of basalt fiber reinforced concrete in comparison with other types of fiber concretes is caused by the chemical resistance of BF in the environment of hardening concrete, the simple technology of introducing fiber into the concrete matrix and the safety of the coating exploitation [35]. Despite this, the use of basalt fiber for reinforcing flexural members remains insufficiently studied to date.

Thus, the relevance of research is due to:

- the presence in the existing methods of calculating the bearing capacity of flexural members, reinforced by the build-up of the compressed zone of concrete with various methods of processing the surface of old concrete, a large number of assumptions and empiricism with static and dynamic loading;
- insufficient knowledge of the compatibility of the work of old and new concrete, with different methods of processing the surface of the reinforcement structure, during bending; the values of abrasion of the reinforcement layer have not been practically investigated, which is the most important characteristic for layered elements that perceive flexural stresses;
- the need for further development of methods for calculating the bearing capacity of bent reinforced concrete elements when reinforcing structural elements by increasing the compressed concrete zone.

The aim of the work is to study the reinforcement of flexural elements of reinforced concrete members with basalt-fiber reinforced mortar (BFM).

2. Materials and Methods

2.1. Methods

A theoretical justification of the interaction of the BFM reinforcement layer with traditional concrete, technological factors during layer-by-layer concreting of coatings, as well as substantiation of the influence of various properties of the components of basalt-fiber reinforced mortars on monolithic coatings during the operation was carried out [36]. Verification and refinement of theoretical conclusions are confirmed by laboratory and production experiments [37]. The variable composition and quality of the components of the basalt-fiber-reinforced mortar mix are additional factors that, together with technological factors, determine the final properties of special-purpose layers from the BFM [38]. The creation of a monolithic multilayer structure with specified physical and mechanical properties requires an integrated approach in research, which consists in establishing the features of the interaction of layers, structure formation of concrete under different hardening conditions, the relationship between the structure of concrete and the physicochemical processes of cement hydration and structure formation of cement paste in the BFM [39].

The stiffness of basalt-fiber mortar mixes was determined using a time (in seconds) of complete settling of the mix on a vibrating table. Specimens of $40 \times 40 \times 160$ mm^3 in size (for flexural studies) and $100 \times 100 \times 100$ mm^3 (for compression studies) were made. Six specimens of each composition and size were made. Compressive strength testing of concrete specimens was carried out according to Russian State Standard GOST 10,180 using an IP 1250 hydraulic press (ZIPO, Lipetsk, Russia). Flexural strength of the specimens was tested on a hydraulic press (Testing, Berlin, Germany) according to Russian State Standard GOST 310.4-81.

Testing of concrete by a LKI-3 abrasion wheel (ZIPO, Lipetsk, Russia) was carried out on specimens with a size of $100 \times 100 \times 100$ mm^3 according to Russian State Standard GOST 13087-2018. The lower edge of the specimen was abraded. Before testing, the samples were weighed and the area of the abraded edge was measured. Simultaneously, two specimens were tested on the abrasion circle. A concentrated vertical force (300 ± 5) N was applied to each specimen (in the center), which corresponded to a pressure of (60 ± 1) kPa. After installing the specimens and applying an abrasive to the abrasive disk (uniform layer of (20 ± 1) g of grinding grain), the wheel drive was turned on and abrasion was performed. Every 30 m of the abrasion path passed by the specimens (28 revolutions), the abrasion disk was stopped. Remains of abrasive material and concrete powder were removed from it and a new portion of abrasive was poured onto it and the abrasive drive was turned on again. This operation was repeated five times, which constituted one test cycle (150 m of the test path). After each test cycle, the specimens were removed from the nest, turned 90° in the horizontal plane (around the vertical axis), and the following test cycles were carried out. In total, four test cycles were carried out for each specimen, the total abrasion path was 600 m. After four test cycles, the samples were removed from the nests, wiped with a dry cloth and weighed.

The study of frost resistance was carried out in accordance with the Russian state standard GOST 10,060 on specimens of $100 \times 100 \times 100$ mm^3. The specimens were immersed in water, first at 1/3 of the height for a day, then at 2/3 of the height for a day, and then completely immersed in water for two days. Then the specimens were placed into a CV-105S freezer (Polair, Moscow, Russia) at a temperature of -18 °C. Each freezing cycle lasted 2.5 h, the thawing cycle at 20 °C was carried out for 2 h. The frost resistance grade was evaluated by the value of the compressive strength after a certain number of freeze-thaw cycles.

2.2. Materials

To ensure the physical and mechanical properties that meet the current standards, the selection of the composition of the basalt fiber mortar mix was checked. For this purpose, control prismatic specimens of the proposed layered structure with dimensions of $100 \times 100 \times 400$ mm^3 with the specified physical and mechanical properties were made. The composition of the basalt-fiber mortar mix for a production experiment with a reinforcement layer is given in Table 1.

Table 1. Consumption of mix components for the BFM, kg/m^3.

Portland Cement M_c	Sand M_s	BF M_f	Water M_w
472.1	1416.3	113.3	198.3

Portland cement CEM I 42.5 N (Belgorod cement, Belgorod, Russia) was used as a binder. Quartz sand with a fraction of 1.25 mm (Belgorod sand, Belgorod, Russia) was used as a fine aggregate. The appearance and technical characteristics of fiber used are given in Figure 1 and Table 2.

Figure 1. Basalt fiber appearance obtained by optical microscopy.

Table 2. Technical characteristics of the basalt fiber used.

Tensile strength, MPa	197.1
Fiber diameter, mm	165×10^{-3}
Fiber length, mm	110 ± 2.5
Elastic modulus, GPa	75
Elongation ratio, %	3.2
Melting temperature, °C	1450
Resistant to alkalis and corrosion	high
Density, kg/m^3	2750

Basalt fiber mortar mixes require the following conditions in the process of mix preparation: the required amount of equally high-strength basalt fibers; during the technological process, basalt fiber must retain a significant part of its strength; fibers must have good adhesion to mortar and concrete; uniform distribution of basalt fiber throughout the entire volume of the matrix, while they should not be in direct contact with each other; basalt fiber should have a higher modulus of elasticity compared to the matrix. Fulfillment of the listed conditions requires technological measures of different content and complexity. The components of the basalt-fiber reinforced mortar mix are dosed with an accuracy of

1% by weight batchers used in factories for the production of ready-mixed concrete or precast concrete.

2.3. Mix Design

As factors of influence at various stages of the study of the composition of the reinforcement layer were taken: a sand to cement ratio M_s/M_c; a water to cement ratio M_w/M_c; a content of basalt fiber μ_s, in% of the sand weight; stiffness of the BFM mix (Table 3). The studied factors of the composition of the BFM reinforcement layer were taken as follows: BF content, mix homogeneity, degree and duration of compaction, and physical and mechanical properties (axial compressive and flexural strength, frost resistance and abrasion), as well as the interaction of layers and their stable balance.

Table 3. Experiment planning matrix.

	Planning Matrix		
Mix ID	**Sand to Cement Ratio M_s/M_c**	**Water to Cement Ratio M_w/M_c**	**Content of Basalt Fiber μ_s**
1	5	0.70	16
2	1	0.70	16
3	5	0.40	16
4	1	0.40	16
5	5	0.70	0
6	1	0.70	0
7	5	0.40	0
8	1	0.40	0
9	5	0.55	8
10	1	0.55	8
11	3	0.70	8
12	3	0.40	8
13	3	0.55	16
14	3	0.55	0
15	3	0.55	8
16	3	0.55	8
17	3	0.55	8

3. Results and Discussion

3.1. Creation of an Analysis Model

In world practice, there are two methods for constructing multilayer rigid layers of reinforcement of floor slabs: according to the splicing scheme, when structural and technological measures are used to "glue" the coating layers, and according to the build-up scheme, when the sliding of the coating layers relative to each other is ensured. The most inexpedient application of the splicing method is due to the high labor intensity and the presence of a large number of through cracks in the lower layer after a certain time of the coating operation. On the other hand, in the design plan, the coatings built by the splicing method do not fundamentally differ from single-layer when calculating the effect of operational loads. The BFM reinforcement layer technology ensures reliable adhesion of the layers, and the bearing capacity of the multilayer system practically does not differ from the corresponding single-layer monolithic one. In this case, the design moment can be determined by the formulas for calculating single-layer floor slabs, based on the value of the characteristics of the layered coating [40–43].

When calculating the thickness of the BFM reinforcement layer, it was proceeded from the solutions of structural mechanics for slabs. For slabs, this condition is expressed by the general differential equation [44,45].

$$D\left(\frac{\partial^4 \omega}{\partial x^4} + 2\frac{\partial^2 \omega}{\partial x^2 \partial y^2} + \frac{\partial^4 \omega}{\partial y^4}\right) = P_0(x,\, y) + q_0(x,\, y) \tag{1}$$

where ω—slab deflection; x, y—coordinates of the middle plane of the slab; $P_0(x, y)$—normal response function; $q_0(x, y)$—external load function; D—cylindrical stiffness of the slab $D = \frac{E_b\, t^3}{2(1-v^2)}$; E_b, v—respectively, the modulus of elasticity and Poisson's ratio of the slab material; t—slab thickness.

The method for solving problems of the operation of multilayer coatings under the influence of operational loads was taken as the basis for substantiating the design scheme and principles of designing layers from dispersed reinforced concrete of the reinforcement layer in the study. It simplifies, if possible, the model prerequisites for describing the operation of layers, where the bearing layers are represented by classical Kirchhoff-Love plates. In this case, when solving problems, the maximum possible number of design features of coatings is taken into account and, in combination with appropriate experimental studies, the method allows us to consider the whole variety of coatings designs and meet the needs of their practical application.

As a design scheme, a model was adopted, according to which the planned operational loads affect the floor slab with a reinforcement layer from the BFM. It has believed that the layers do not peel off from each other during deformation. Within each layer, elastic modulus, density and thickness are constant, but not the same for different layers. These hypotheses, together with Hooke's law, make it possible to obtain well-known formulas for the forces acting on a rectangular element of the wear layer from the BFM.

The calculation of multilayer slabs according to the Kirchhoff-Love theory is typical for slabs with a ratio of thicknesses of rigid layers of 1:1, since it allows one to determine the stress-strain state of a slab from the action of bending moments caused by a vertical load. The influence of horizontal loads in calculating the strength of a multilayer slab structure is not taken into account by the existing methods and regulations, since the growth of longitudinal tangential stresses along the depth of the upper layer of reinforcement from the BFM is slower than the very effect on this layer of the vertical load.

The stress in the BFM amplification layer is determined by the formula [45,46]:

$$\begin{cases} \sigma_x = \frac{\partial^2 \phi}{\partial y^2} - \frac{E \cdot z}{1-v^2}\left(\frac{\partial^2 u_z}{\partial x^2} + v\frac{\partial^2 u_z}{\partial y^2}\right) \\ \sigma_y = \frac{\partial^2 \phi}{\partial x^2} - \frac{E \cdot z}{1-v^2}\left(\frac{\partial^2 u_z}{\partial y^2} + v\frac{\partial^2 u_z}{\partial x^2}\right) \\ \tau_{x,y} = -\frac{\partial^2 \phi}{\partial x \partial y} - \frac{E \cdot z}{1-v^2}\frac{\partial^2 u_z}{\partial x \partial y} \end{cases} \tag{2}$$

where φ—stress function; u_z—displacement by horizontal forces.

To numerically implement the adopted model and find the values of deflections ω of the slab structures and displacements u of the reinforcement layer, SCAD software is used.

3.2. Experimental Part

The production of a reinforcement BFM layer includes technological processes for the preparation, transportation, laying and distribution of the mix into the coating, its processing, care of the laid concrete and curing until the demolding strength.

The issues of introducing fibers into mortar are of great importance. High-quality production of a fiber-reinforced mortar can be achieved provided that a uniform and gradual supply of BFM to the concrete mixer is ensured while the components of the basalt-fiber concrete mixture are mixed in it. The homogeneity of the mix and the strength of the concrete are greatly influenced by the mixing time. In case of insufficient duration of concrete mixing, the homogeneity of the concrete deteriorates and its strength decreases. An increase in the mixing time beyond the optimal one (the strength of concrete increases, but extremely insignificantly) negatively affects the properties of the BFM. This is due to the fact that an increase in the mixing time of the basalt fiber mortar mix leads to a decrease in the reinforcing effect of basalt fiber (the ratio of the fiber length to its diameter) due to the mechanical action on the fiber and its crushing. The optimum mixing time can only be determined experimentally.

In slab reinforcement layer technology, the most important task is to achieve maximum layer density and a strong bond with old concrete.

According to [47], for basalt fiber concrete mixes, the vibration amplitude should be within 0.5 mm for vibrating bars with a vibration frequency of 50 Hz (3000 per min). Large vibration amplitudes (A = 1–2 mm) without weights cause loosening of the basalt fiber concrete mix and worsen the properties of the BFM.

It is known that the physical and mechanical properties of concrete also depend on the voidness of the aggregates and its changes during the preparation of mortar mixes [48,49]. Previous studies [47] show that when the sand is saturated with fiber, the porosity of the mix decreases until the optimum degree of saturation is reached (with the BF content μ_s = 8% of the sand mass). After that, the decrease in the porosity of the mix ceases, and with a further increase in the BF content, its growth is observed, characterized by an excess amount of the mix that did not enter the measuring vessel. Then a moment comes when the porosity of the basalt fiber-reinforced concrete mix turns out to be greater than the porosity of the original sand and lumps are formed from the interwoven BF (when the BF content μ_s > 16% of the sand mass). This can be explained by the fact that when the BF content is $\mu_s \leq$ 8% of the mass of sand, in the process of compaction, BFs are additional vibration centers, occupy part of the voids in the sand, and are composited more densely than sand without BF. With an increase in the content of BF 8 < $\mu_s \leq$ 16% of the mass of sand, BF forms spatial frameworks in the sand, thereby worsening compaction and increasing the porosity of the basalt fiber mortar. It is known that the porosity of the basalt fiber mortar mainly depends on the voidness of the original sand, while the porosity of the basalt fiber mortar remains constant regardless of the type of sand.

The results of studies of the duration of vibration treatment of coatings using the BFM reinforcement layers, depending on the stiffness of the basalt fiber mortar mixture, according to the experiment planning matrix and 17 points of the plan, are given in Table 4. The duration of vibration treatment was measured using a stopwatch with an accuracy of 1 s in a series of 6 specimens. The specimens were made according to the developed research methodology, in accordance with the plan for the laboratory experiment.

Table 4. Influence of vibration treatment on mix stiffness.

Mix ID	Mix Stiffness According to the Russian Standard GOST 10181.1-81 t_q, s	Duration of Vibration Treatment of the Mix t, s	Ratio between the Duration of Vibration Treatment of the Mix and Its Stiffness t/t_q
1	<4	-	-
2	44	111	2.52
3	6	15	2.50
4	37	94	2.54
5	<4	-	-
6	26	66	2.54
7	5	12	2.40
8	38	94	2.47
9	<4	-	-
10	42	104	2.48
11	8	20	2.50
12	34	86	2.53
13	28	69	2.46
14	24	62	2.58
15	21	53	2.52
16	20	50	2.50
17	22	55	2.50

The prepared basalt fiber mortar was unloaded from the concrete mixer and layer-by-layer, according to the plan of the experiment, was placed in metal molds, which were fixed on the vibration platform (Figure 2a). The molds were preliminarily lubricated from

the inside with machine oil with a layer of about 0.5 mm. During the first 30 s of vibration, all mold nests were uniformly filled with solution (Figure 2b). For the complete filling of the form, the total vibration time was 1.5 min. The excess solution was removed with a wiped with a damp cloth with a knife at a slight angle to the surface and smoothed with light pressure.
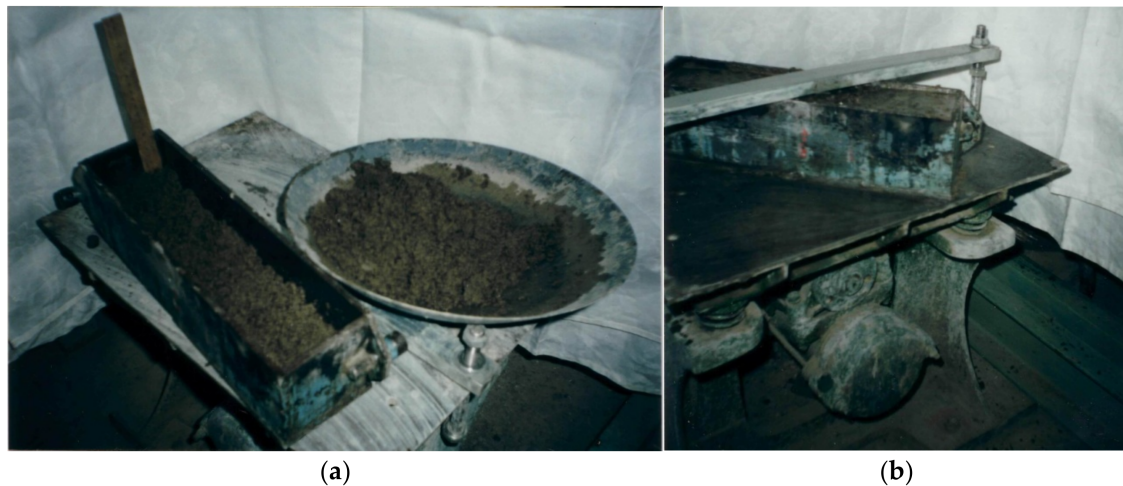

(**a**)　　　　　　　　　　　　　　　　　　　(**b**)

Figure 2. Preparing BFM specimens: (**a**) laying in metal molds; (**b**) Form compacting within the first 30 s of vibration.

The required degree of compaction of coatings with special-purpose layers made of BFM is ensured when using vibrating platforms with an oscillation amplitude of A = 0.3–0.5 mm and a frequency of f = 75–50 Hz, and the compaction duration t depends on the stiffness of the basalt fiber-reinforced concrete mix t_q and is $t = 2.5t_q$.

The results of the investigated factors are presented in Table 5.

Table 5. Mechanical properties and performances.

Mix ID	Flexural Strength, MPa	Compressive Strength, MPa	Frost Resistance, Cycles	Abrasion, g/cm^2
1	5.3	10.4	21	0.301
2	9.6	28.9	279	0.062
3	2.4	4.1	41	0.585
4	8.8	38.9	295	0.099
5	2.8	15.7	37	0.209
6	5.2	26.2	79	0.175
7	1.1	4.2	3	0.398
8	4.7	32.3	76	0.157
9	4.4	5.2	238	0.455
10	9.6	28.8	376	0.171
11	7.6	17.5	330	0.148
12	6.2	21.3	328	0.274
13	10.2	27.8	256	0.181
14	4.2	21.5	120	0.174
15	9.1	22.2	339	0.216
16	8.9	22.1	333	0.217
17	8.8	22.4	338	0.216

After two years of operation, a survey of the reinforcement layer of the floor slabs was carried out (Figure 3), based on the results of which a defective statement was drawn up (Table 6).

Figure 3. Defect picture.

Table 6. List of defects.

Defect	Approximate Number of Defective Slabs, %
Peeling surface	-
Separate sinks	1
Transverse cracks	2
Longitudinal cracks	2
Cracks at an angle to the axis	1
Shrinkage cracks	-
Chipped seam edges	1

Using the MatLab software, regression equations are obtained for calculating the physical and mechanical properties of the coating specimens:

- Compressive strength (Figure 4)

$$R_c = 50.12 - 13.71(M_s/M_c) + 14.73(M_w/M_c) - 0.42\mu_s - 0.63(M_s/M_c)^2 - 69.39(M_w/M_c)^2 + 0.078\mu_s{}^2$$
$$+ 19.52(M_s/M_c)(M_w/M_c) - 0.11\mu_s(M_s/M_c) - 0.82\mu_s(M_s/M_c), \text{MPa}; R^2 = 0.95$$
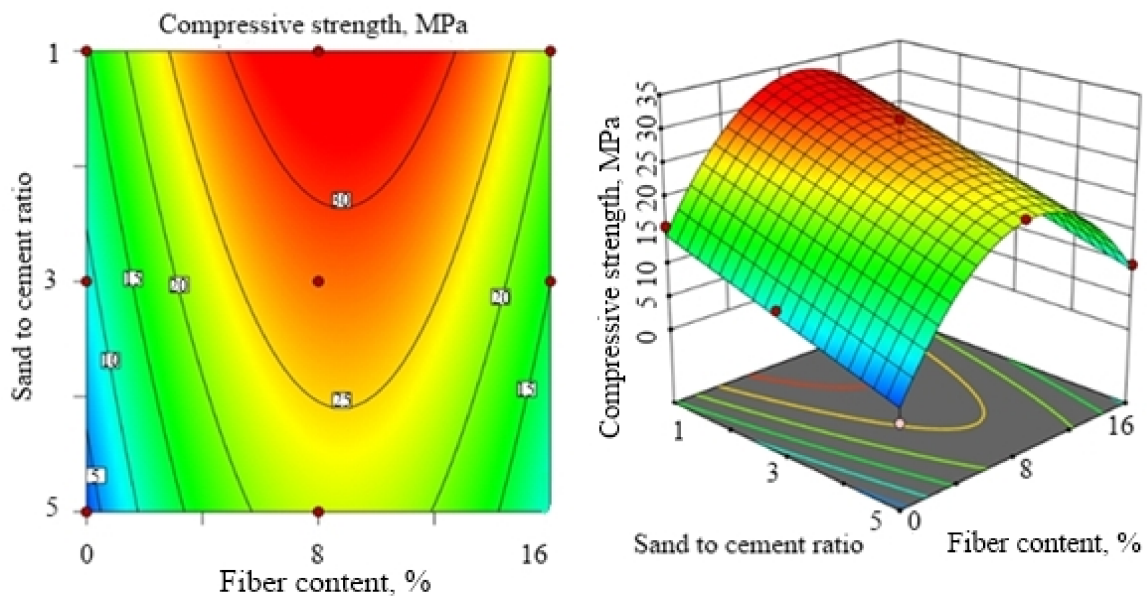
Figure 4. Compressive strength response surface at water to cement ratio of 0.55.

- Flexural strength (Figure 5)

$$R_f = -16.7 + 031(M_s/M_c) + 92.81(M_w/M_c) - 0.087\mu_s - 0.43(M_s/M_c)^2 - 92.86(M_w/M_c)^2 + 0.0057\mu_s^2$$
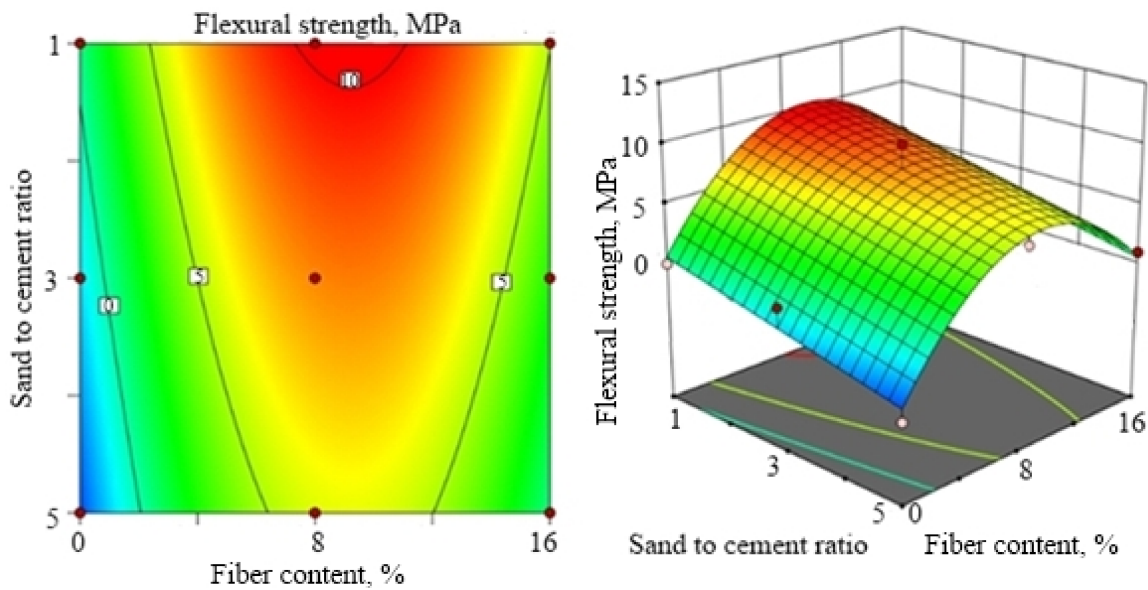$$+ 2.41(M_s/M_c)(M_w/M_c) - 0.006\mu_s(M_s/M_c) - 0.23\mu_s(M_s/M_c), \text{MPa}; R^2 = 0.94$$

Figure 5. Flexural strength response surface at water to cement ratio of 0.55.

- Frost resistance (Figure 6)

$$F = -146.34 + 69.95(M_s/M_c) + 602.56(M_w/M_c) + 74.771\mu_s - 15.38(M_s/M_c)^2 - 497.17(M_w/M_c)^2 - 3.126\mu_s^2$$
$$+ 9.84(M_s/M_c)(M_w/M_c) - 3.927\mu_s(M_s/M_c) - 11.021\mu_s(M_s/M_c), \text{cycles}; R^2 = 0.96$$
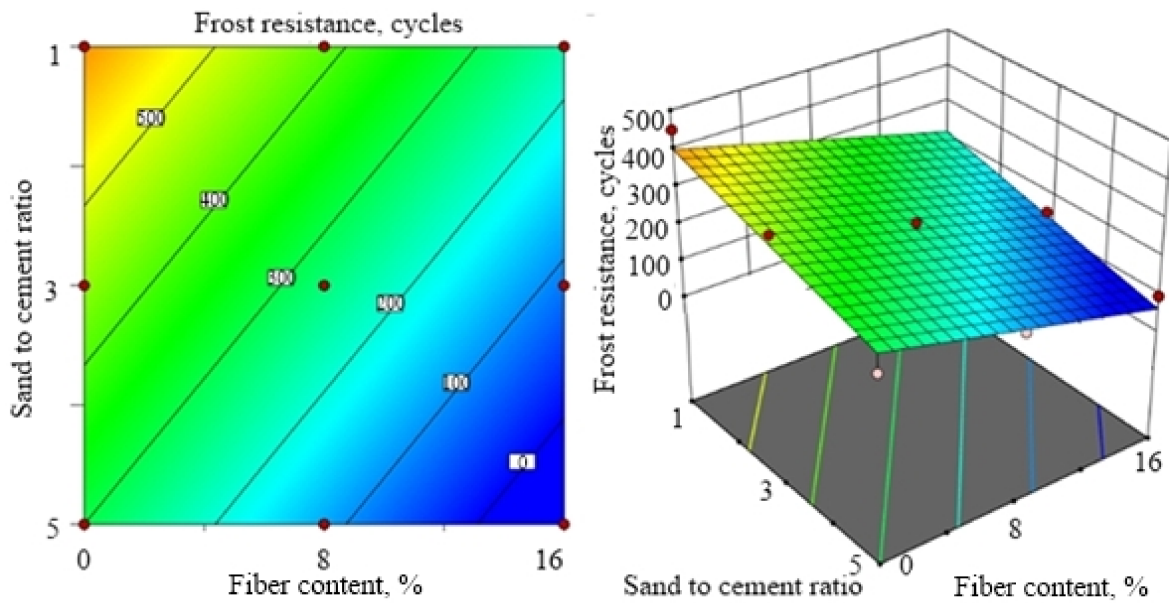
Figure 6. Frost resistance response surface at water to cement ratio of 0.55.

- Abrasion (Figure 7)

$$A = -0.02 + 0.002(M_s/M_c) + 0.51(M_w/M_c) + 0.014\mu_s + 0.031(M_s/M_c)^2 - 0.54(M_w/M_c)^2 - 0.0006\mu_s^2$$
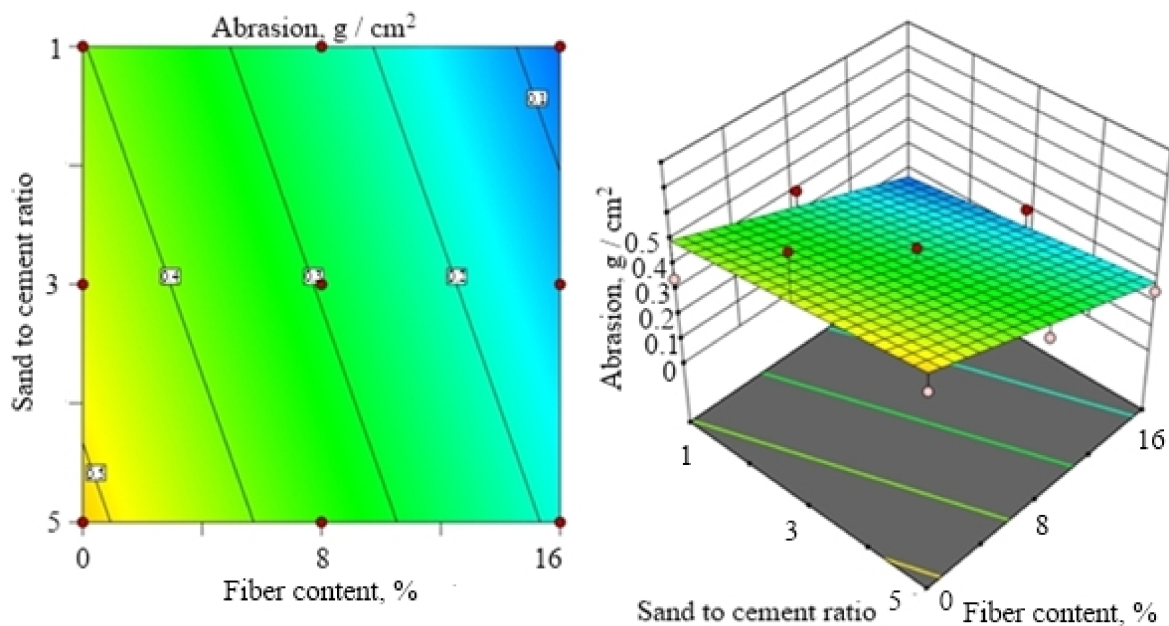$$- 0.17(M_s/M_c)(M_w/M_c) + 0.0027\mu_s(M_s/M_c) - 0.008\mu_s(M_s/M_c), g/cm^2; R^2 = 0.95$$

Figure 7. Abrasion response surface at water to cement ratio of 0.55.

Thus, the experimental and theoretical methods were adopted as the main research ones. There are based on theoretical studies of the interaction of a layer of the BFM reinforcement from with traditional concrete and technological factors in layer-by-layer concreting of coatings.

As a result of the economic calculations, it was revealed that the introduction of the proposed technology makes it possible to completely eliminate the consumption of reinforcing steel; reduce energy consumption by 8–10%, as well as decrease the cost of coating production by 20–30%. In addition, harmful emissions of products of electric or gas welding into the atmospheric air are excluded due to their complete reduction.

4. Conclusions

As a result of the study, the criteria for assessing the state of floor slab structures were identified. Conclusions on the state and further work of elements of reinforced concrete structures are considered. Solutions to the problem of reinforcing flexural elements of reinforced concrete structures using a fiber-reinforced concrete layer are described, with particular emphasis on reinforcing floor elements with increased operating requirements. A technique has been developed for constructing a reinforcement layer using fiber-reinforced concrete from basalt fiber. A method for solving problems of the operation of multilayer coatings under the influence of operational loads is used, in which the model prerequisites for describing the operation of layers are simplified, where the bearing layers are represented by classical Kirchhoff-Love plates. When solving problems, the maximum possible number of design features of bending elements is taken into account, in combination with the corresponding experimental studies, the method allows us to consider the whole variety of structures for reinforcing coatings and meet the needs of their practical application. Based on the study of physical and mechanical characteristics, regression equations were obtained and graphical dependences of their change on the content of basalt fiber were constructed. It has been established that with a content of basalt fiber of $4\% \leq \mu_s \leq 16\%$ of the mass of fine aggregate, the axial compression strength is 10–30% higher, and the flexural strength is several times higher in comparison with traditional concretes [50–53]. This allows to assert the optimality of the developed composition and its suitability for strengthening building elements.

Author Contributions: Conceptualization, D.K.; methodology, S.K., Y.B., N.V., and D.B.; software, R.F.; validation, Y.V., D.K., S.K., and R.F.; resources, Y.B., N.V., S.K., and R.F.; writing—original draft preparation, D.B., R.F., S.K., N.V., and D.K.; writing—review and editing, Y.V., S.K., N.V., and Y.B.; visualization, D.B., R.F., N.V., and Y.V.; supervision, S.K. All authors have read and agreed to the published version of the manuscript.

Conflicts of Interest: The authors declare no conflict of interest.

References

1. Betti, M.; Galano, L.; Vignoli, A. Comparative analysis on the seismic behaviour of unreinforced masonry buildings with flexible diaphragms. *Eng. Struct.* **2014**, *61*, 195–208. [CrossRef]
2. Tolstoy, A.D.; Lesovik, V.S.; Glagolev, E.S.; Krymova, A.I. Synergetics of hardening construction systems. *IOP Conf. Ser. Mater. Sci. Eng.* **2018**, *327*, 032056. [CrossRef]
3. Ayzenshtadt, A.; Lesovik, V.; Frolova, M.; Tutygin, A.; Danilov, V. Nanostructured Wood Mineral Composite. *Procedia Eng.* **2015**, *117*, 45–51. [CrossRef]
4. Karpov, D. The algorithm of complex diagnostics of technical condition of building structures on thermograms analysis. *Constr. Mater. Prod.* **2020**. [CrossRef]
5. Monaldo, E.; Nerilli, F.; Vairo, G. Basalt-based fiber-reinforced materials and structural applications in civil engineering. *Compos. Struct.* **2019**, *214*, 246–263. [CrossRef]
6. Penttila, H.; Rajala, M.; Freese, S. Building Information Modelling of Modern Historic Buildings. In Proceedings of the Predicting the Future, 25th eCAADe Konferansı, Frankfurt am Main, Germany, 26–29 September 2007.
7. Birjukov, A.; Bolotin, S. Construction of Temporary Accommodation Camp and Selection of Optimal Type of Building. *Appl. Mech. Mater.* **2015**, *725–726*, 105–110. [CrossRef]
8. Raczkiewicz, W.; Wójcicki, A. Implementation and usage aspects for floors in the residential houses. *E3S Web Conf.* **2018**, *49*, 00085. [CrossRef]
9. Semančík, M. Mausoleum in Horné Obdokovce. *Archit. Urban.* **2007**, *41*, 55–64.
10. Al-Qaraghuli, H.; Alsayed, Y.; Almoghazy, A. Postwar City: Importance of Recycling Construction and Demolition Waste. *IOP Conf. Ser. Mater. Sci. Eng.* **2017**, *245*, 82062. [CrossRef]
11. Fediuk, R.; Smoliakov, A.; Stoyushko, N. Increase in composite binder activity. *IOP Conf. Ser. Mater. Sci. Eng.* **2016**, *156*, 012042. [CrossRef]
12. Lesovik, V.; Voronov, V.; Glagolev, E.; Fediuk, R.; Alaskhanov, A.; Amran, Y.M.; Murali, G.; Baranov, A. Improving the behaviors of foam concrete through the use of composite binder. *J. Build. Eng.* **2020**, *31*, 101414. [CrossRef]

13. Fediuk, R.S.; Lesovik, V.S.; Liseitsev, Y.L.; Timokhin, R.A.; Bituyev, A.V.; Zaiakhanov, M.Y.; Mochalov, A.V. Composite binders for concretes with improved shock resistance. *Mag. Civ. Eng.* **2019**, *85*, 28–38. [CrossRef]

14. Fediuk, R.S. Mechanical Activation of Construction Binder Materials by Various Mills. *IOP Conf. Ser. Mater. Sci. Eng.* **2016**, *125*, 012019. [CrossRef]

15. Fediuk, R.; Pak, A.; Kuzmin, D. Fine-Grained Concrete of Composite Binder. *IOP Conf. Ser. Mater. Sci. Eng.* **2017**, *262*, 012025. [CrossRef]

16. Chernysheva, N.V.; Lesovik, V.S.; Drebezgova, M.Y.; Shatalova, S.V.; Alaskhanov, A.H. Composite Gypsum Binders with Silica-containing Additives. *IOP Conf. Ser. Mater. Sci. Eng.* **2018**, *327*, 032015. [CrossRef]

17. Haridharan, M.K.; Matheswaran, S.; Murali, G.; Abid, S.R.; Fediuk, R.; Mugahed Amran, Y.H.; Abdelgader, H.S. Impact response of two-layered grouted aggregate fibrous concrete composite under falling mass impact. *Constr. Build. Mater.* **2020**, *263*, 120628. [CrossRef]

18. Aghdasi, P.; Ostertag, C.P. Tensile fracture characteristics of Green Ultra-High Performance Fiber-Reinforced Concrete (G-UHP-FRC) with longitudinal steel reinforcement. *Cem. Concr. Compos.* **2020**, *114*, 103749. [CrossRef]

19. Taheri, M.; Barros, J.A.; Salehian, H. Integrated approach for the prediction of crack width and spacing in flexural FRC members with hybrid reinforcement. *Eng. Struct.* **2020**, *209*, 110208. [CrossRef]

20. Attar, H.S.; Esfahani, M.R.; Ramezani, A. Experimental investigation of flexural and shear strengthening of RC beams using fiber-reinforced self-consolidating concrete jackets. *Structures* **2020**, *27*, 46–53. [CrossRef]

21. Katz, A. Properties of concrete made with recycled aggregate from partially hydrated old concrete. *Cem. Concr. Res.* **2003**, *33*, 703–711. [CrossRef]

22. Fediuk, R.; Yushin, A. Composite binders for concrete with reduced permeability. *IOP Conf. Ser. Mater. Sci. Eng.* **2016**, *116*, 012021. [CrossRef]

23. Fediuk, R.S.; Ibragimov, R.A.; Lesovik, V.S.; Pak, A.A.; Krylov, V.V.; Poleschuk, M.M.; Stoyushko, N.Y.; Gladkov, N.A. Processing equipment for grinding of building powders. *IOP Conf. Ser. Mater. Sci. Eng.* **2018**, *327*, 042029. [CrossRef]

24. Feduik, R. Reducing permeability of fiber concrete using composite binders. *Spec. Top. Rev. Porous Media* **2018**, *9*, 79–89. [CrossRef]

25. Rackauskaite, E.; El-Rimawi, J. A Study on the Effect of Compartment Fires on the Behaviour of Multi-Storey Steel Framed Structures. *Fire Technol.* **2015**, *51*, 867–886. [CrossRef]

26. Bhoir, A.S.; Patil, S.P. Effect of post-installed rebar connection on concrete structure. *Int. J. Sci. Technol. Res.* **2019**, *8*, 1045–1050.

27. Martinola, G.; Meda, A.; Plizzari, G.A.; Rinaldi, Z. Strengthening and repair of RC beams with fiber reinforced concrete. *Cem. Concr. Compos.* **2010**, *32*, 731–739. [CrossRef]

28. Lukuttsova, N. Water films (nanofilms) in cement concrete deformations. *Int. J. Appl. Eng. Res.* **2015**, *10*, 35120–35124.

29. Motter, C.J.; Abdullah, S.A.; Wallace, J.W. Reinforced Concrete Structural Walls without Special Boundary Elements. *ACI Struct. J.* **2018**, *115*, 723–733. [CrossRef]

30. Klyuev, S.V.; Klyuev, A.V.; Khezhev, T.A.; Pukharenko, Y.V. High-strength fine-grained fiber concrete with combined reinforcement by fiber. *J. Eng. Appl. Sci.* **2018**, *13*, 6407–6412. [CrossRef]

31. Afroughsabet, V.; Ozbakkaloglu, T. Mechanical and durability properties of high-strength concrete containing steel and polypropylene fibers. *Constr. Build. Mater.* **2015**, *94*, 73–82. [CrossRef]

32. Klyuev, S.V.; Klyuev, A.V.; Shorstova, E. Fiber Concrete for 3-D Additive Technologies. *Mater. Sci. Forum* **2019**, *974*, 367–372. [CrossRef]

33. Frazão, C.; Camões, A.; Barros, J.; Gonçalves, D. Durability of steel fiber reinforced self-compacting concrete. *Constr. Build. Mater.* **2015**, *80*, 155–166. [CrossRef]

34. Niaki, M.H.; Fereidoon, A.; Ahangari, M.G. Experimental study on the mechanical and thermal properties of basalt fiber and nanoclay reinforced polymer concrete. *Compos. Struct.* **2018**, *191*, 231–238. [CrossRef]

35. Feduik, R.S.; Smoliakov, A.K.; Timokhin, R.A.; Batarshin, V.O.; Yevdokimova, Y.G. Using thermal power plants waste for building materials. *IOP Conf. Ser. Earth Environ. Sci.* **2017**, *87*, 092010. [CrossRef]

36. Ragavendra, S.; Reddy, I.P.; Dongre, A. Fibre Reinforced Concrete—A Case Study. In Proceedings of the 33rd National Convention of Architectural Engineers and National Seminar on "Architectural Engineering Aspect for Sustainable Building Envelopes" ArchEn, BuilEn-2017, by Institution of Engineers Indian in Association with Indian Association of Structural Engineers at: Institution of Engineers Khairatabad, Khairtabad, India, 10–11 November 2017.

37. Safdar, M.; Matsumoto, T.; Kakuma, K. Flexural behavior of reinforced concrete beams repaired with ultra-high performance fiber reinforced concrete (UHPFRC). *Compos. Struct.* **2016**, *157*, 448–460. [CrossRef]

38. Sim, J.; Park, C.; Moon, D.Y. Characteristics of basalt fiber as a strengthening material for concrete structures. *Compos. Part B Eng.* **2005**, *36*, 504–512. [CrossRef]

39. High, C.; Seliem, H.M.; El-Safty, A.; Rizkalla, S.H. Use of basalt fibers for concrete structures. *Constr. Build. Mater.* **2015**, *96*, 37–46. [CrossRef]

40. Farzad, M.; Shafieifar, M.; Azizinamini, A. Experimental and numerical study on bond strength between conventional concrete and Ultra High-Performance Concrete (UHPC). *Eng. Struct.* **2019**, *186*, 297–305. [CrossRef]

41. Zhu, D.; Liu, S.; Yao, Y.; Li, G.; Du, Y.; Shi, C. Effects of short fiber and pre-tension on the tensile behavior of basalt textile reinforced concrete. *Cem. Concr. Compos.* **2019**, *96*, 33–45. [CrossRef]

42. Burkeev, D.O.; Romanova, A.I.; Murafa, A.A.; Maksimchuk, O.V.; Voronin, A.V. Improving the efficiency and mobility of urban housing maintenance services. *IOP Conf. Ser. Mater. Sci. Eng.* **2020**, *786*, 012028. [CrossRef]

43. Carette, J.; Staquet, S. Monitoring and modelling the early age and hardening behaviour of eco-concrete through continuous non-destructive measurements: Part II. Mechanical behaviour. *Cem. Concr. Compos.* **2016**, *73*, 1–9. [CrossRef]

44. Sorelli, L.G.; Meda, A.; Plizzari, G.A. Steel fiber concrete slabs on ground: A structural matter. *ACI Struct. J.* **2006**, *103*, 551–558. [CrossRef]

45. Zhu, Y.; Zhang, Y.X. Nonlinear finite element analyses of FRP-reinforced concrete slabs using a new layered composite plate element. *Comput. Mech.* **2010**, *46*, 417–430. [CrossRef]

46. Vecchio, F.; Tata, M. Approximate analyses of reinforced concrete slabs. *Struct. Eng. Mech.* **1999**, *8*, 1–18. [CrossRef]

47. Adamczyk, W.P.; Górski, M.; Ostrowski, Z.; Bialecki, R.; Kruczek, G.; Przybyła, G.; Krzywon, R.; Bialozor, R. Application of numerical procedure for thermal diagnostics of the delamination of strengthening material at concrete construction. *Int. J. Numer. Methods Heat Fluid Flow* **2019**, *30*, 2655–2668. [CrossRef]

48. Regelink, I.C.; Stoof, C.R.; Rousseva, S.; Weng, L.; Lair, G.J.; Kram, P.; Nikolaidis, N.P.; Kercheva, M.; Banwart, S.; Comans, R.N. Linkages between aggregate formation, porosity and soil chemical properties. *Geoderma* **2015**, *247–248*, 24–37. [CrossRef]

49. Poon, C.; Shui, Z.; Lam, L. Effect of microstructure of ITZ on compressive strength of concrete prepared with recycled aggregates. *Constr. Build. Mater.* **2004**, *18*, 461–468. [CrossRef]

50. Klyuyev, S.V.; Klyuyev, A.V.; Sopin, D.M.; Netrebenko, A.V.; Kazlitin, S.A. Heavy loaded floors based on fine-grained fiber concrete. *Mag. Civ. Eng.* **2013**, *38*, 7–14. [CrossRef]

51. Usanova, K.; Barabanshchikov, Y.G. Cold-bonded fly ash aggregate concrete. *Mag. Civ. Eng.* **2020**, *95*, 104–118. [CrossRef]

52. Petrovna, L.N.; Germanovna, L.I.; Gennadievich, K.E. High-Performance Fine Concrete Modified with Nano-Dispersion Additive. *Int. J. Appl. Eng. Res.* **2014**, *9*, 16725–16731.

53. Salamanova, M.; Bataev, D.; Uzayeva, A.; Gacayev, Z. Recipes of Knitting Systems Alkaline Activation Using Natural Raw Materials of the Chechen Republic. *Mater. Sci. Forum* **2020**, *1011*, 1–7. [CrossRef]